metals

MDPI

Article

# Microstructure and Mechanical Properties of Dissimilar Friction Stir Welding between Ultrafine Grained 1050 and 6061-T6 Aluminum Alloys

**Yufeng Sun [1,2,*], Nobuhiro Tsuji [2] and Hidetoshi Fujii [1]**

[1] Joining and Welding Research Institute, Osaka University, Ibaraki 5670047, Japan; fujii@jwri.osaka-u.ac.jp
[2] Department of Materials Science and Engineering, Kyoto University, Kyoto 6068501, Japan; nobuhiro-tsuji@mtl.kyoto-u.ac.jp
* Correspondence: yfsun@jwri.osaka-u.ac.jp; Tel.: +81-6-68798663; Fax: +81-6-687-986-53

Academic Editor: Giuseppe Casalino
Received: 25 August 2016; Accepted: 15 October 2016; Published: 21 October 2016

**Abstract:** The ultrafine grained (UFGed) 1050 Al plates with a thickness of 2 mm, which were produced by the accumulative roll bonding technique after five cycles, were friction stir butt welded to 2 mm thick 6061-T6 Al alloy plates at a different revolutionary pitch that varied from 0.5 to 1.25 mm/rev. In the stir zone, the initial nano-sized lamellar structure of the UFGed 1050 Al alloy plate transformed into an equiaxial grain structure with a larger average grain size due to the dynamic recrystallization and subsequent grain growth. However, an equiaxial grain structure with a much smaller grain size was simultaneously formed in the 6061 Al alloy plates, together with coarsening of the precipitates. Tensile tests of the welds obtained at different welding speeds revealed that two kinds of fracture modes occurred for the specimens depending on their revolutionary pitches. The maximum tensile strength was about 110 MPa and the fractures were all located in the stir zone close to the 1050 Al side.

**Keywords:** ultrafine grained structure; dissimilar friction stir welding; dynamic recrystallization; aluminum alloy

## 1. Introduction

As a solid state joining process, friction stir welding (FSW) was invented by the welding insitute TWI in the UK with the original purpose to weld light metals such as aluminum and magnesium alloys, which has been demonstrated to be very difficult by traditional fusion welding methods [1,2]. Since FSW is performed at a temperature lower than the melting point of the materials to be welded, FSW can produce joints with fewer defects or porosity, low residual stresses, etc., compared with other fusion welding methods [3,4]. The FSW technique has developed very rapidly since its emergence and it has now been expanded to many high melting point metallic materials, including Cu, Ti, Fe, stainless steels, and even high carbon steels, which were considered to be unweldable materials by fusion welding methods because of the formation of the brittle martensite phase [5–8]. Therefore, with the increasing effort to improve fuel efficiency in industry, the use of the FSW technique must be in strong demand in the near future for the welding of light materials, especially aluminum and magnesium alloys.

Recently, the FSW of certain types of ultrafine grained (UFGed) materials has been investigated. UFGed materials are those that generally have an average grain size of less than 1 μm. UFGed materials have an increased length of grain boundaries acting as obstacles for moving dislocation and therefore exhibit superior properties at ambient temperature to their coarse grained counterparts, which also makes them attractive candidates for a range of potential applications in the automotive,

aerospace and biomedical industries. There are many severe plastic deformation (SPD) techniques like accumulative roll bonding (ARB), equal channel angular pressing (ECAP), and high pressure torsion (HPT) to produce UFGed metallic materials, among which the ARB technique can be used to produce UFGed materials in bulk plate form [9]. The welding or joining of UFGed materials is therefore becoming more and more important. Obviously, the UFGed materials cannot be welded by the general fusion welding methods, since the molten pool generated during the welding process will inevitably destroy the UFGed structure and result in a much coarser grain size in the solidified butt. The UFGed alloys like the 1050, 1100, 6016 Al alloys and IF steel prepared by the ARB technique have also been successfully subjected to the FSW process [10–15]. It was revealed that a hardness reduction did take place in the FSW processed materials with the UFGed structure due to the coarsening of the grain size. Although the initial UFGed structure is still very difficult to be retained in the stir zone, the degradation of the mechanical properties was significantly reduced.

However, the dissimilar FSW involved with UFGed materials has never been reported according to the best of our knowledge. The FSW of dissimilar alloys has been significantly studied including dissimilar aluminum alloys, Al/Mg alloys, Al/Steel pairs, etc. The main salient feature of FSW of dissimilar metals and alloys is thought to be the variation in asymmetry or the degree of symmetry with reference to the weld centerline [16]. For example, Lee et al. evaluated the joint microstructure of the dissimilar welds between cast A356 and wrought 6051 aluminum alloys produced at various welding speeds [17]. Palanivel et al. [18] studied the effect of the tool rotational speed and pin profile on the microstructure and tensile strength of dissimilar FSW between the AA5083-H111 and AA6351-T6 aluminum alloys. They found that joint strength was affected due to the variations in the materials behavior. It is evident that an important aspect in the FSW of dissimilar materials is the selection of the appropriate alloys for the advancing and the retreating sides to obtain the optimum mixing and weld properties due to the asymmetric material flow in the joints. It was found that the maximum tensile strength was achieved for the dissimilar FSW AA2024/AA7075 aluminum alloy joints only when the 2024 Al alloy was located on the advancing side [19]. Kwon et al. successfully obtained Al/Mg dissimilar FSW joints when the AZ31 alloy and Al alloy were located on the RS and AS, respectively. However, the reason of the work-piece configuration was not explained in detail [20]. According to the investigation of dissimilar FSW between Al and Cu alloys, the suitable configuration and even the amount of offset of the tool from the joint centerline were considered to play an important role in obtaining high joints properties [21–23]. More recently, Sun et al. conducted the dissimilar spot FSW between the UFGed 1050Al and 6061-T6 aluminum alloys [24]. However, the UFGed materials have not been reported to be dissimilar FSW processed with other materials.

In this study, the dissimilar friction stir butt welding was carried out between the UFGed 1050 Al and 6061-T6 aluminum alloys in order to expand the application of UFGed materials. After welding, the microstructure and mechanical properties of the joints were characterized and discussed.

## 2. Materials and Methods

In this study, the dissimilar FSW was performed between 2 mm thick UFGed 1050 Al and commercial 6061-T6 Al alloy plates. The UFGed 1050 Al alloy plates were fabricated by the ARB process after 5 cycles. The 6061-T6 Al alloy has a yielding strength of about 266 MPa and the UFGed 1050 Al has a yielding strength of about 200 MPa, much higher than the 75 MPa of coarse grained 1050 Al alloys. Prior to the dissimilar FSW, the two kinds of Al plates were cleaned with acetone to remove any impurities on the surface such as dirt and oil. To optimize the welding conditions, the UFGed Al plates were separately placed on the advancing side (AS) and retreating side (RS). The rotating tools were made of tool steel, which had a concave-shaped shoulder geometry with a diameter of 12 mm and a threaded probe with a diameter of 4 mm and a length of 1.8 mm. The tool axis was tilted by 3° with respect to the normal direction of the sample surface. During welding, the rotating tool exactly penetrated into the butt interface between the two dissimilar materials at a speed of 0.5 mm/s. After the shoulder of the tool touched the plate surface, the tool started to travel

along the butt interface and left a weld seam behind. The welding was carried out at a constant load of 8000 kN and a constant rotation speed of 800 rpm, while the welding speed was varied at 400, 600, 800 and 1000 mm/min, corresponding to the revolutionary pitch (welding speed/rotation speed) of 0.5, 0.75, 1 and 1.25 mm/rev, respectively.

After welding, optical microscopy (OM, Olympus Microscopy, Tokyo, Japan, BX51M) and scanning electronic microscopy (SEM, JEOL Microscopy, Osaka, Japan, JEOL-7001FA) with an electron backscattered diffraction (EBSD, TSL Solutions, Tokyo, Japan) system were used to characterize the microstructure of the joints. For the OM observations, the specimens were first mechanically polished and then chemically etched with Keller's reagent. The specimens for the EBSD measurement were electro-polished using a solution of $HNO_3$:$CH_4O$ = 3:7 at 15 V and −30 °C. The Vickers micro-hardness tests on the cross-sectional plane of the joints were carried out at an interval of 0.5 mm using a testing machine (AAV500, Akashi, Tokyo, Japan). The tensile tests of the joints were carried out using a testing machine (5500, Instron, Norwood, MA, USA) with a cross-head speed of 1 mm/min.

## 3. Results and Discussion

Figure 1 shows the microstructure of the two types of base metals. The UFGed 1050 aluminum alloys have a lamellar structure with an average lamellar width of about 300 nm as shown in Figure 1a, which is the typical microstructure of the ARB processed materials. These lamellar shaped grains normally have a boundary spacing or grain width much smaller than 1 μm. In addition, the elongated grains in the ARB processed materials are generally surrounded by high angle boundaries, a grain misorientation angle larger than 15°, and high fraction of high angle boundaries of more than 70%. The 6061-T6 aluminum alloys have a coarse equiaxial grain structure with an average grain size of about 18 μm as shown in Figure 1b. As a typical precipitate hardened aluminum alloy, the mechanical properties of the 6061 Al alloy slightly depend on the grain size of the alloy, but are strongly dominated by the volume fraction, size and distribution of the strengthening precipitates. The 6061 alloy under T6 heat treatment consists of a high density of needle-shape precipitates and a low density of β-$Mg_2Si$ precipitates [25].

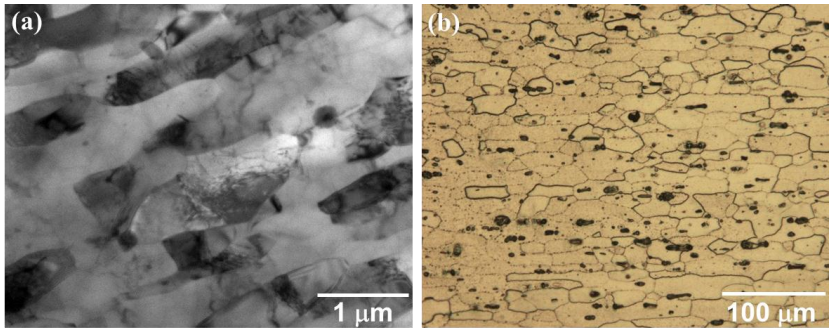


**Figure 1.** The microstructure of the base metal of (**a**) ultrafine grained (UFGed) 1050 aluminum and (**b**) 6061-T6 aluminum alloys.

Figure 2 is the photos of the samples produced by FSW at different revolutionary pitches, in which the UFGed 1050 and 6061-T6 aluminum plates were placed on the AS and RS side, respectively. It was found that the dissimilar FSW between these two materials could never been successful. During every welding process, a large defect was formed in the UFGed 1050 aluminum plates and the defect became larger when decreasing the welding speed, as shown in the figures. It was noted that the dissimilar FSW between two aluminum alloys might be difficult since they have quite different deformation characteristics at high temperature. Because the rotating tool on the AS shows the same direction of self-rotation and traveling along the butt interface, the material in the AS generally experiences a higher strain rate and higher temperature than that in the RS [26,27]. Therefore, the materials with a

low melting point are usually placed on the RS during the dissimilar welding process between two materials with quite different melting points, for example, dissimilar FSW between aluminum and steel alloys [28,29]. Sometimes the rotating tool also needs to be offset from the butt interface toward the lower melting temperature materials in order to prevent tool wear or overheating of the lower melting materials. In this study, although the 1050 and 6061 aluminum alloys had very similar melting points, the UFGed 1050 aluminum had a very unstable microstructure, which easily resulted in the dynamic recrystallization and subsequent grain growth at elevated temperature during the welding process. When the UFGed 1050 Al plate was placed on the AS, the materials became very soft and would flow into the RS with the rotation of the tool. However, the 6061 Al on the RS was still hard to be plasticized due to the relatively lower temperature and strain rate. The softened 1050 Al could not be stirred into the 6061 Al on the RS and finally was extruded outside stir zone. As a result, a defect was formed on the AS due to the insufficient amount of the materials. Therefore, placing the UFGed materials on the AS was not suitable for the dissimilar FSW in this study.

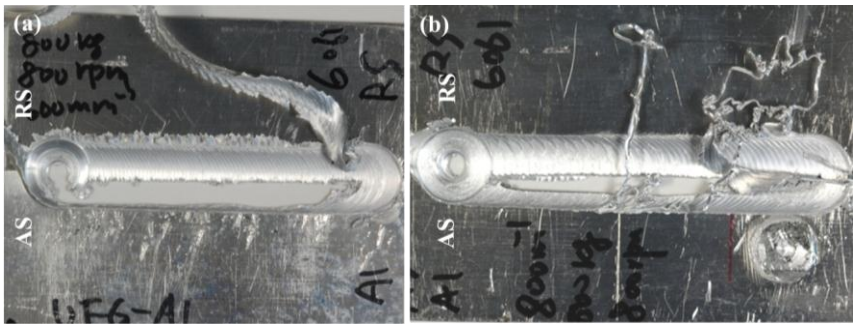


**Figure 2.** Photo showing the appearance of the dissimilar friction stir welding (FSW) joints with UFGed 1050Al on the advancing side (AS) and 6061-T6 on the retreating side (RS) produced at a revolutionary pitch of (**a**) 0.75 mm/rev; and (**b**) 1 mm/rev.

Figure 3 shows photos of the samples produced at different welding speeds, in which the UFGed 1050 Al and 6061-T6 Al alloys were placed on the RS and AS, respectively. The welding was successfully done at the wide revolutionary pitches from 0.5 to 1.25 mm/rev and no obvious defects could be observed based on the appearance of the joints as shown in Figure 3a,b. However, it was found that at a larger revolutionary pitch of speed of 1 or 1.25 mm/rev, the width of the welding seam became smaller and smaller with the increasing welding distance. It was proposed that the heat input was not sufficient at the higher welding speed during welding process, and the rotating tool could not penetrate deep enough to make the tool shoulder touch the sample surface completely. As a result, a lack of contact between the tool shoulder and the surface of the work-piece was formed, as shown by the arrow in Figure 3d. Due to the very different material flow of the two materials, the interface could still be observed on the surface of the joint centerline. At the lower revolutionary pitch of less than 0.75 mm/rev, the welding process became very stable and a homogeneous welding seam was obtained, except that a slightly more flash formed on the retreating side of the joint welded at a revolutionary pitch of 0.5 mm/rev. It was revealed that the FSW of dissimilar aluminum alloys should be conducted with suitable locations and in this study the UFGed aluminum plates should be put on the RS.

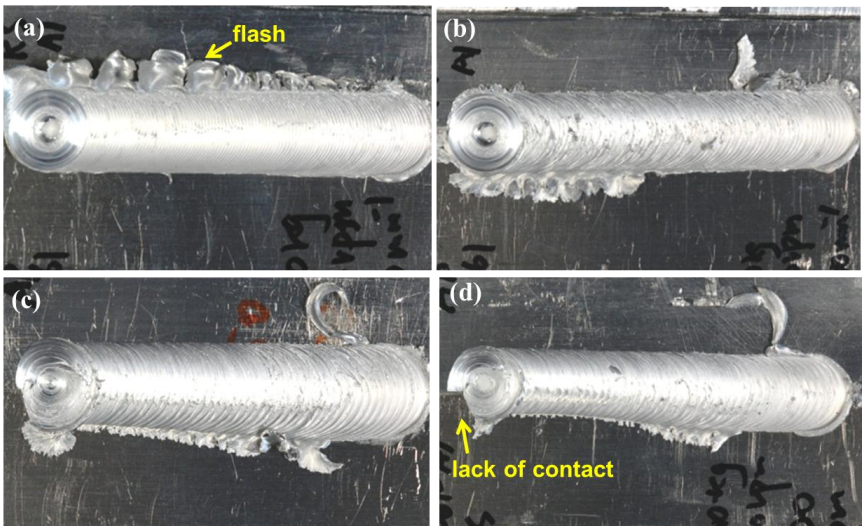


**Figure 3.** Photo showing the appearance of the dissimilar FSW joints with UFGed 1050Al on the RS side and 6061-T6 on the AS produced at a revolutionary pitch of (**a**) 0.5; (**b**) 0.75; (**c**) 1; and (**d**) 1.25 mm/rev.

Figure 4 shows the cross-sectional macrostructure of the dissimilar FSW joints between the UFGed 1050 Al and 6061-T6 Al alloy plates, which were obtained at different revolutionary pitches ranging from 0.5 to 1.25 mm/rev. Since the 6061-T6 Al alloy was etched black using Keller's reagent, the interface and mixing status of the two materials could be readily discerned in the joints. The entire stir zone of the FSW joint consists of the shoulder-affected zone and probe-affected zone. The shoulder affected zone becomes larger at higher rotation speed or lower welding speed, while the probe affected zone shows less sensitive to the welding condition. This has been recently confirmed by the investigation with an adjustable rotating tool [30]. As a result, a crown-like stir zone is generally formed along the transverse direction, especially for thin plates like in this study. It can be found that the area of the stir zone became larger with the decreasing welding speed for all the samples. At higher revolutionary pitch of 1 and 1.25 mm/rev, the bending of the interface between the alternative layers of the aluminum sheets was observed in the UFGed 1050 Al side near the stir zone as shown by the arrow in Figure 4c. Generally, a well chemically etched cross-section of the friction stir weld reveals an onion-ring structure in the stir zone with a round flow pattern formed by bright and dark lamellae in the dissimilar aluminum joints [31,32]. However, in this study the round flow pattern containing bright and dark lamellae was not observed in the stir zone, probably due to the relatively smaller thickness of the plates. In contrast, roughly two kinds of mixing types could be classified. One was the mixing of dissimilar materials caused by the lower heat input at the high revolutionary pitches of 1 and 1.25 mm/rev. In this case, the size of the stir zone was small and only several prismatic blocks of the 6061 alloy were found in the stir zone. Most of the stir zone was composed of the 1050 Al alloys probably due to its lower viscosity than 6061 alloy at high temperature. In addition, the TMAZ/SZ boundary close to the 6061 Al side was very sharp and nearly vertical, which indicated that the probe-affected zone was very limited due to the fast traveling speed. The other kind of mixing was caused by the higher heat input at the lower revolutionary pitches of 0.75 and 0.5 mm/rev. The shoulder affected zone became much larger and expand downward to the probe affect zone. The material flow of the two materials in the stir zone was stronger and the boundary between the TMAZ/SZ near the 6061-T6 Al side declined more to the base metal. As a result, more material of the 6061-T6 Al alloy was plastically deformed and pushed into the stir zone. Especially, at the low revolutionary pitch of 0.5 m/rev, the two materials could not be easily discerned any more in the stir zone due to the severe mechanical mixing by the rotating tool.

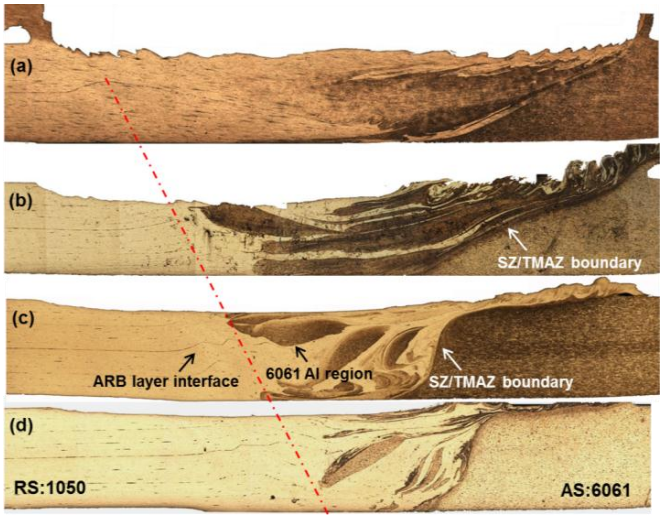


**Figure 4.** Optical microscopy (OM) images showing the cross-sectional macrostructure of the UFGed 1050/6061-T6 Al alloys dissimilar FSW joints produced at the different revolutionary pitches of (**a**) 0.5; (**b**) 0.75; (**c**) 1; and (**d**) 1.25 mm/rev.

Figure 5 shows the enlarged OM images of the stir zone of the dissimilar FSW joints produced at the different welding speeds. In all the figures except for Figure 5d, the white and black areas indicated the 1050 Al and the 6061 Al alloys, respectively. As shown in Figure 4, only several large blocks of the 6061 Al alloys were mixed in the stir zone at the high welding speed. Figure 5a,b show the boundary between the 6061 Al blocks and the surrounding 1050 Al produced at the revolutionary pitches of 1.25 and 1 mm/rev, respectively. A couple of small welding defects could be distinguished at the corner of the 6061-T6 region. The formation of the defects might be caused by the insufficient plastic deformation at the lower heat input. In addition, it is interesting to note that deformed UFGed 1050 Al layers were observed to be mixed in the region of the 6061-T6 aluminum alloy. In most of the large 6061-T6 blocks, a large number of small segments of white color, which corresponded to the 1050 Al alloy were observed. However, the 6061-T6 aluminum materials were never found to be distributed inside the 1050 Al area. When the revolutionary pitch decreased to 0.75 mm/rev, the mixing of the two materials became much stronger. However, large stripe-like areas of the two different materials were still alternatively distributed together as shown in Figure 5c. When the revolutionary pitch further decreased to 0.5 mm/rev, the mixing became quite complete and the two different materials could not be easily discerned under by OM observation, as shown in Figure 5d.

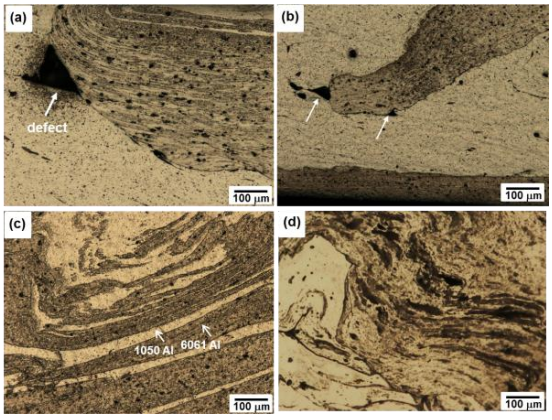


**Figure 5.** OM images showing the microstructure of the stir zone of the dissimilar FSW joints obtained at the different revolutionary pitches of (**a**) 1.25; (**b**) 1; (**c**) 0.75; and (**d**) 0.5 mm/rev.

To reveal how the two materials were mixed in the stir zone, SEM observations of the cross-sectional microstructure of the joints were carried out. As a typical example, Figure 6 shows the microstructure of the joints produced at a revolutionary pitch of 0.75 mm/rev. In most parts of the area it showed a very high density of white particles, while in the other parts particles were hardly observed. From the element mapping by Energy Dispersive X-ray Spectroscopy EDS measurement as shown in Figure 7, the particles were confirmed to be the $Mg_2Si$ phase. The coarsening of the $Mg_2Si$ particles in the 6061 Al alloy area due to the quite high heat input generated during the FSW process, was also observed in the FSW of similar 6xxx aluminum alloys [33]. The distribution of particles in the 6061-T6 Al alloy made it easy to be distinguished from the area of the 1050 Al, which contained no particles. The 1050 Al part was like a long stripe with a width of about 10 μm in the mixture of the two materials, which was very likely caused by the flow stress during welding. Figure 6b shows the boundary between the 6061 and 1050 Al alloys. The $Mg_2Si$ particles were found distributed on the boundary, which played a role in pinning of the migration of the grain boundary during the welding process. In addition, sub-grains with the average size of several nanometers were formed inside the 6061 Al grains, which were also found in the dissimilar friction stir spot welding between UFGed 1050 and 6061-T6 Al alloys [24].

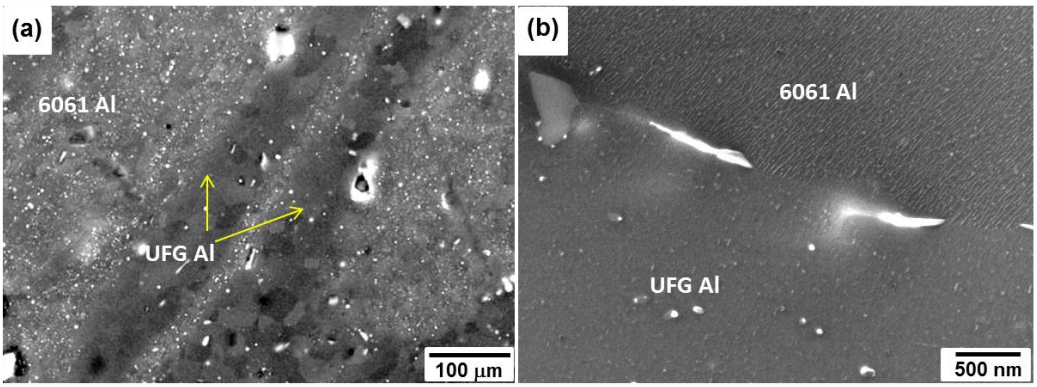


**Figure 6.** SEM (scanning electronic microscopy) images showing the mixing of the two kinds of aluminum alloys in the stir zone. (**a**) Alternative layered structure of the two materials; (**b**) interfacial microstructure between the UFGed 1050/6061-T6 aluminum alloys.

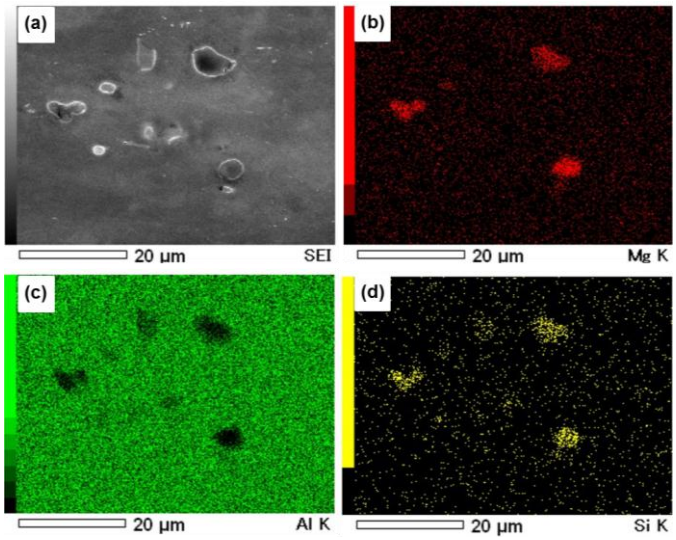


**Figure 7.** The EDS mapping showing the $Mg_2Si$ particles distributed in the area of the 6061 Al alloy. (**a**) SEM image and corresponding distribution of (**b**) Mg; (**c**) Al; and (**d**) Si elements.

Figure 8 shows the EBSD maps measured in the mixed area of the stir zone, in which only the high angle boundary larger than 15° was plotted. The black area in the maps indicated the distribution of the coarsened $Mg_2Si$ precipitates due to the generated Kikuchi pattern with a low confidence index (CI) value. Figure 8a shows the EBSD-IPF map of the mixed area in the stir zone of the joint produced at a revolutionary pitch of 0.75 mm/rev. An obvious bimodal structure containing two types of grains with quite different grain size could be observed. One type of grain structure had a larger average grain size of about 2.6 μm, while the other type of grain structure had a smaller average grain size of about 1.1 μm. Figure 8b shows the corresponding image quality (IQ) map, in which the matrix of the 6061 Al alloy contains additional elements like Mg and Cu and therefore its crystalline lattice deviated from that of the pure Al. Another reason for the low IQ value of the 6061 Al region might be caused by the formation of a high density of subgrain, in which the density of dislocation might be higher. Therefore, the area with the larger grain size corresponded to the 1050 Al alloys, while the area with the smaller grain size corresponded to the 6061 Al alloys. Figure 8c,d shows the IPF and IQ map of the joint produced at a revolutionary pitch of 0.5 mm/rev, when a higher heat was generated during welding. The mixing of the two materials became stronger; however, it still can be distinguished due to their quite different grain size and IQ value. In this case, the average grain size of the 1050 Al and 6061 Al were 4.5 and 1.5 μm, respectively. With the increase in the heat input during welding, the grain growth of the 1050 Al increases faster than that of the 6061 Al alloys.

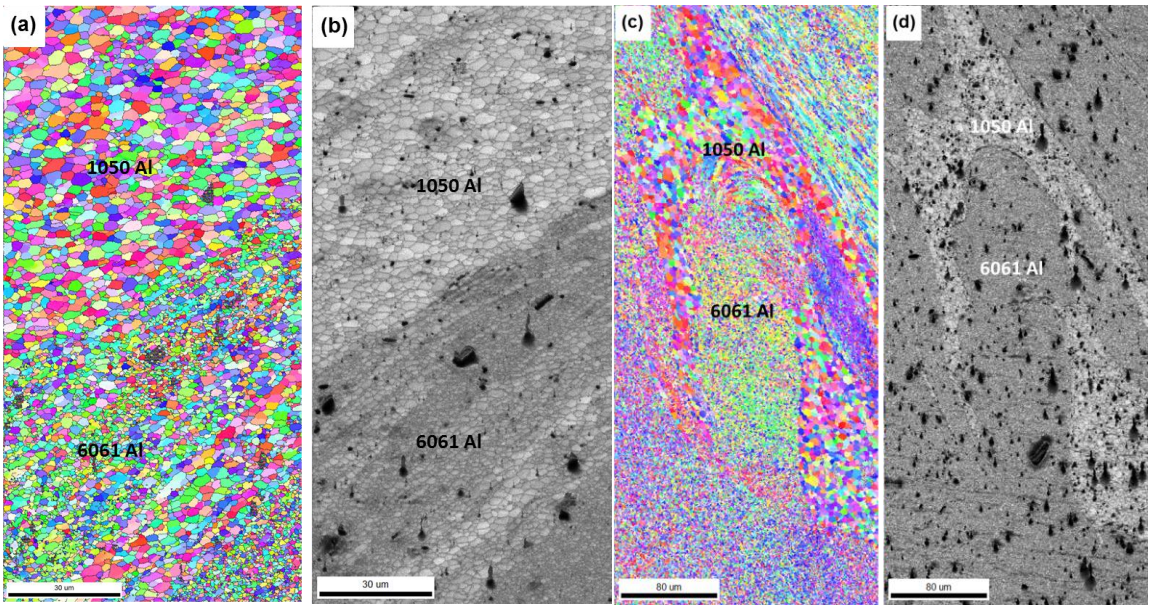


**Figure 8.** Electron backscattered diffraction (EBSD) map showing the microstructure of the stir zone of the dissimilar FSW joint produced at the revolutionary pitches of (**a**) and (**b**) 0.75 mm/rev; (**c**) and (**d**) 0.5 mm/rev.

It is interesting to note that in the stir zone the 1050 Al showed an average grain size quite larger than 300 nm of the BM, while the 6061 Al showed a fairly refined microstructure compared with that 18 μm of the BM. In addition, both 1050 Al and 6061Al had equiaxial grain structure and large fraction of high angle grain boundary, indicating the occurrence of dynamic recrystallization. Because FSW is a kind of high strain rate plastic deformation at high temperature, the evolution of the grain structure in the stir zone during the FSW strongly depends on the initial microstructure such as the grain boundary structure, grain size, dislocation density, etc., of the base metal [34]. Usually, when the FSW process is applied to the conventional metals or alloys, a very refined microstructure will be formed in the stir zone of the joints. The grain refinement process is generally believed to be driven by the grain subdivision or the continuous dynamic recrystallization, termed geometric dynamic

recrystallization which was first recognized by Humphreys and McQeen [35–37]. The continuous dynamic recrystallization is characterized by a strain-induced progressive rotation of the subgrains with little boundary migration during the FSW process and is prone to occur at grain boundary in aluminum alloys with a high level of solute like Mg and Zn, by progressive lattice rotation.

The pure Al alloy has a high stacking fault energy and the UFGed 1050 Al produced by the SPD process generally showed a fairly unstable microstructure upon heat treatment. That is because unlike conventional metals or alloys, the as-ARB processed materials contain a large quantity of vacancies and dislocations generated by the severe plastic deformation. Therefore, the UFGed alloys are very likely to be structurally recovered at a relatively low temperature to decrease the defect density within the grains. At the same time, continuous grain growth took place and the mean grain size increased. Similarly, during the dissimilar FSW process in this study, the area of the 1050 Al showed a fairly coarse grain structure, which resulted in an obvious hardness reduction in the stir zone.

Figure 9 shows the microhardness profile for the dissimilar FSW joints produced at different welding speeds. The variation in the hardness value corresponded to the typical microstructural zones. For all the specimens, the base metal of both the UFGed 1050 and 6061-T6 Al alloys showed the highest value. From the BM to HAZ, a gradual decrease in microhardness was observed for both materials. For the 6061-T6 alloy, the decrease was due to the accelerated solid solution of precipitates and the simultaneous occurrence of coarsening of particles caused by the weld thermal cycles. However, the stir zone also showed some regions with a high hardness value similar to that of the base metal, which was caused by the significantly refined grain size, while in the UFG 1050 Al side, the decrease in the hardness was mainly caused by the grain growth and the dislocation density.

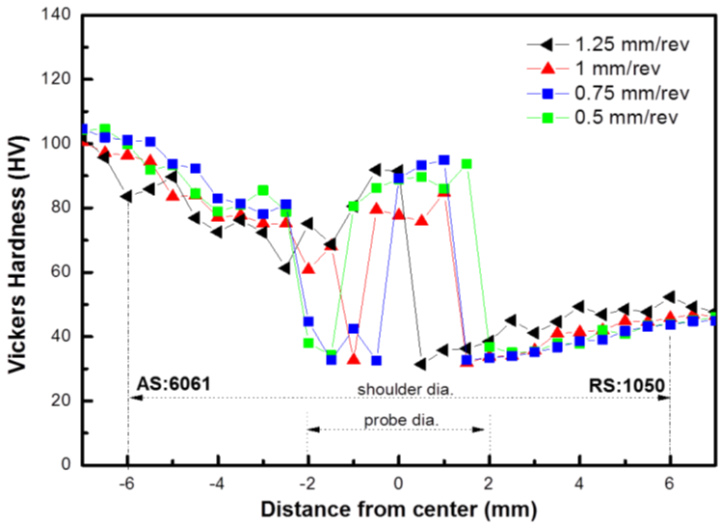


**Figure 9.** Hardness profile along center line of the cross-sectional plane of the dissimilar FSW joints produced at various welding speeds.

Figure 10 shows the tensile strain-stress curves of the specimens produced at different welding speed. For the specimens produced at the revolutionary pitches of 1.25 and 1 mm/rev, both the tensile strength and elongation were lower than the other specimens produced at the smaller revolutionary pitches. It is proposed that the mixing of the two materials was not sufficient and several large blocks of different materials were formed in the stir zone. In addition, a couple of defects with several micrometers in size were found at the corner of the 6061-T6 aluminum block that may more or less decrease the strength of the joints. When the revolutionary pitch decreased to 0.75 or 0.5 mm/rev, the high heat input enhanced the plastic deformation and therefore led to further mixing of the two materials in the stir zone. The microstructure of the stir zone also became more homogeneous. As a result, the tensile strength and elongation increased to about 110 MPa and 13% for the sample welded

at 0.75 mm/rev and 110 MPa and 22.5% for the sample welded at 0.5 mm/rev. The largest joint efficient was therefore about 55% with respect to the UFG 1050 Al base metal. However, the joints strength was still much larger than the ultimate strength of the commercial coarse grain structured 1050 Al alloy. However, too much heat input in the joints produced at 0.5 mm/rev resulted in serious grain growth of both materials, especially the 1050 Al alloy parts. The tensile strength slightly decreased again, however, with compensation of a much increased elongation.

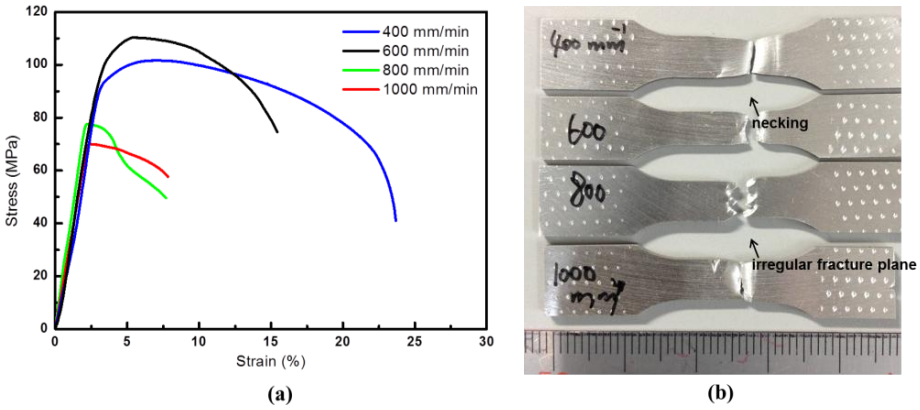


**Figure 10.** (**a**) Tensile strain-stress curves of the dissimilar FSW joints produced at different welding speeds; and (**b**) photo of the fractured specimens after the tensile tests.

From the photos showing the appearance of the fractured tensile specimen, the joints produced at high welding speeds showed a brittle fracture, and even some irregular zigzag edges near the fracture plane could be found. In contrast, the joints produced at a revolutionary pitch of 0.5 mm/rev showed obvious necking near the fractured plane, indicative of ductile failure of the specimen.

Figure 11 shows the morphologies of the fracture plane after tensile testing of the dissimilar FSW joints produced at 1 and 0.5 mm/rev, corresponding to the brittle and ductile kinds of fracture mode. For the specimen produced at 1 mm/rev, several irregular fractured planes were observed as shown in Figure 11a. Some dimple patterns could be found in some of the fracture planes, while some other planes showed tearing of the specimens. For the specimen produced at a welding speed of 0.5 mm/rev, the fracture plane had typical dimple patterns as shown in Figure 11b, indicating ductile failure of the specimen.

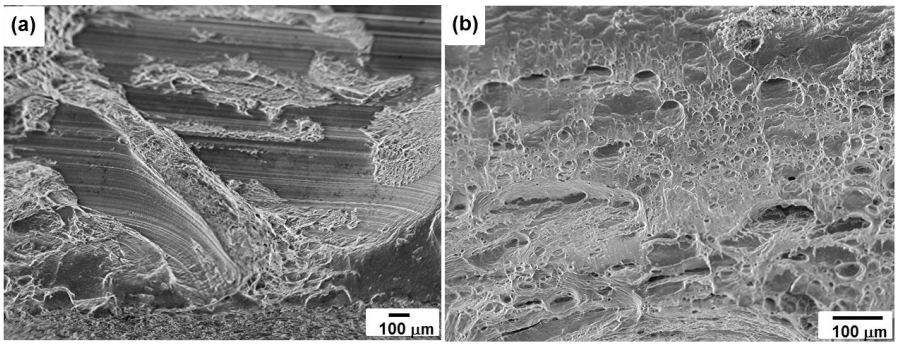


**Figure 11.** SEM images showing the morphologies of the fractured surfaces of the joints produced at a revolutionary pitch of (**a**) 1; and (**b**) 0.5 mm/rev.

## 4. Conclusions

The dissimilar FSW the UFGed 1050 Al to 6061-T6 alloy was successfully performed at the wide revolutionary pitches from 0.5 to 1.25 mm/min; however, this took place only when the 6061-T6 Al

alloy was put on the AS. Otherwise, sound welds could not be obtained due to the large defects formed in the softened 1050 Al side.

The size of the stir zone became larger with the decrease in the revolutionary pitch and the mixing between the two dissimilar Al alloys became much more homogeneous. However, in the entire stir zone of the dissimilar FSW, it was found that the 1050 Al was mixed into the 6061 side. However, no 6061 Al was mixed into the 1050 Al area.

In the stir zone, the two dissimilar Al alloys could still be distinguished. The nano-sized lamellar structure of the UFGed 1050 Al alloy could not be distinguished any more. Finally, the 1050 Al showed dynamic recrystallization and had an average grain size larger than that of the 6061 Al alloy.

All the dissimilar joints fractured in the stir zone during the tensile tests. For the joints produced at 1.25 and 1 mm/rev, the fracture strength was low and showed the brittle fracture mode. In contrast, the joints produced at 0.75 and 0.5 mm/rev showed a higher tensile strength and large plastic elongation.

**Acknowledgments:** The authors wish to acknowledge the financial support of the Collaborative Research Based on Industrial Demand "Heterogeneous Structure Control: Towards Innovative Development of Metallic Structural Materials" by Japan Science and Technology Agency (JST), the Global COE Programs from the Ministry of Education, Sports, Culture, Science, and a Grant-in-Aid for Science Research from the Japan Society for Promotion of Science and Technology of Japan, ISIJ Research Promotion Grant.

**Author Contributions:** Yufeng Sun designed the experiments, performed the experiments, analyzed the data and wrote the paper. Nobuhiro Tsuji and Hidetoshi Fujii provided the alloy sheets, directed the research and contributed to the discussion and interpretation of the results.

**Conflicts of Interest:** The authors declare no conflict of interest.

## References

1. Thomas, W.M.; Nicholas, E.D.; Needhman, J.C.; Church, M.G.; Templesmith, P.; Dawes, C.J. Friction Stir Butt Welding. International Patent Application No. PCT/GB92/02203, 1991.
2. Mishra, R.S.; Ma, Z.Y. Friction stir welding and processing. *Mater. Sci. Eng. R* **2005**, *50*, 1–78. [CrossRef]
3. Luijendijk, L. Welding of dissimilar aluminum alloys. *J. Mater. Process. Technol.* **2003**, *103*, 29–35. [CrossRef]
4. Nandan, R.; Debroy, T.; Bhadeshia, H.K.K.H. Recent advances in friction-stir welding-Process, weldment structure and properties. *Prog. Mater. Sci.* **2008**, *53*, 980–1023. [CrossRef]
5. Sun, Y.F.; Fujii, H. Investigation of the welding parameter dependent microstructure and mechanical properties of friction stir welded pure copper. *Mater. Sci. Eng. A* **2010**, *527*, 6879–6886. [CrossRef]
6. Fujii, H.; Sun, Y.F.; Kato, H. Investigation of welding parameter dependent microstructure and mechanical properties in friction stir welded pure Ti joints. *Mater. Sci. Eng. A* **2010**, *527*, 3386–3391. [CrossRef]
7. Sun, Y.F.; Fujii, H.; Imai, H.; Kondoh, K. Suppression of hydrogen-induced damage in friction stir welded low carbon steel joints. *Corros. Sci.* **2015**, *94*, 88–98. [CrossRef]
8. Fujii, H.; Cui, L.; Maeda, M.; Nogi, K. Effect of tool shape on mechanical properties and microstructure of friction stir welded aluminum alloys. *Mater. Sci. Eng. A* **2006**, *419*, 25–31. [CrossRef]
9. Saito, Y.; Utsunomiya, H.; Tsuji, N.; Sakai, T. Novel ultra-high straining process for bulk materials-development of the accumulative roll-bonding (ARB) process. *Acta Mater.* **1999**, *47*, 579–583. [CrossRef]
10. Lipinska, M.; Olejnik, L.; Pietras, A.; Rosochowski, A.; Bazarnik, P.; Goliński, J.; Brynk, T.; Lewandowska, M. Microstructure and mechanical properties of friction stir welded joints made from ultrafine grained aluminum 1050. *Mater. Des.* **2015**, *88*, 22–31.
11. Topic, I.; Hoppel, H.W.; Goken, M. Friction stir welding of accumulative roll-bonded commercial-purity aluminum AA1050 and aluminum alloy AA6016. *Mater. Sci. Eng. A* **2009**, *503*, 163–166. [CrossRef]
12. Sabooni, S.; Karimzadeh, F.; Enayati, M.H.; Ngan, A.H.W. Recrystallization mechanism during friction stir welding of ultrafine-and coarse-grained AISI 304L stainless steel. *Sci. Tech. Weld. Join.* **2016**, *21*, 287–294. [CrossRef]
13. Sato, Y.S.; Urata, M.; Kokawa, H.; Ikeda, K. Hall-Petch relationship in friction stir welds of equal channel angular-pressed aluminium alloys. *Mater. Sci. Eng. A* **2003**, *354*, 298–305. [CrossRef]
14. Fujii, H.; Ueji, R.; Takada, Y.; Kitahara, H.; Tsuji, N.; Nakata, K.; Nogi, K. Friction stir welding of ultrafine grained interstitial free steel. *Mater. Trans.* **2006**, *47*, 239–242. [CrossRef]
15. Sun, Y.F.; Fujii, H.; Takada, Y.; Tsuji, N.; Nakata, K.; Nogi, K. Effect of initial grain size on the joint properties of friction stir welded aluminum. *Mater. Sci. Eng. A* **2009**, *527*, 317–321. [CrossRef]

16. Murr, L.E. A review of FSW research on dissimilar metal and alloy systems. *J. Mater. Eng. Perform.* **2010**, *19*, 1071–1089. [CrossRef]
17. Lee, W.B.; Yeon, Y.M.; Jung, S.B. The joint properties of dissimilar formed Al alloys by friction stir welding according to the fixed location of materials. *Scr. Mater.* **2003**, *49*, 423–428. [CrossRef]
18. Palanivel, R.; Mathews, P.K.; Murugan, N.; Dinaharan, I. Effect of tool rotational speed and pin profile on microstructure and tensile strength of dissimilar friction stir welded AA5083-H111 and AA6351-T6 aluminum alloys. *Mater. Des.* **2012**, *40*, 7–16. [CrossRef]
19. Khodir, S.A.; Shibayanagi, T. Friction stir welding of dissimilar AA2024 and AA7075 aluminum alloys. *Mater. Sci. Eng. B* **2008**, *148*, 82–87. [CrossRef]
20. Kwon, Y.J.; Shigematsu, I.; Saito, N. Dissimilar friction stir welding between magnesium and aluminum alloy. *Mater. Lett.* **2008**, *62*, 3827–3829. [CrossRef]
21. Tolephih, M.H.; Mahmood, H.M.; Hashem, A.H.; Abdullah, E.T. Effect of tool offset and tilt angle on weld strength of butt joint friction stir welded specimens of AA2024 aluminum alloy welded to commercial pure copper. *Chem. Mater. Res.* **2013**, *3*, 49–58.
22. Carlone, P.; Astarita, A.; Palazzo, G.S.; Paradiso, V.; Squillace, A. Microstructural aspects in Al-Cu dissimilar joining by FSW. *Int. J. Adv. Manu. Technol.* **2015**, *79*, 1109–1116. [CrossRef]
23. Sahu, P.K.; Pal, S.; Pal, S.K.; Jain, R. Influence of plate position, tool offset and tool rotational speed on mechanical properties and microstructures of dissimilar Al/Cu friction stir welding joints. *J. Mater. Proc. Technol.* **2016**, *235*, 55–67. [CrossRef]
24. Sun, Y.F.; Fujii, H.; Tsuji, N. Microstructure and mechanical properties of spot friction stir welded ultrafine grained 1050 Al and conventional grained 6061-T6 Al alloys. *Mater. Sci. Eng. A* **2013**, *585*, 17–24. [CrossRef]
25. Sato, Y.S.; Urata, M.; Kokawa, H. Parameters controlling microstructure and hardness during friction stir welding of precipitation-Hardenable Aluminum alloy 6063. *Metall. Mater. Trans. A* **2002**, *33*, 625–635. [CrossRef]
26. Maeda, M.; Liu, H.J.; Fujii, H.; Shibayanagi, T. Temperature Field in the vicinity of FSW-Tool during friction stir welding of aluminum alloys. *Weld. World* **2005**, *49*, 69–75. [CrossRef]
27. Liu, H.; Fujii, H.; Maeda, M.; Nogi, K. Heterogeneity of mechanical properties of friction stir welded joints of 1050-H24 aluminum alloy. *J. Mater. Sci. Lett.* **2003**, *22*, 441–444. [CrossRef]
28. Yasui, T.; Ishii, T.; Shimoda, Y.; Tsubaki, M.; Fukumoto, M.; Shinoda, T. Friction stir welding between aluminum and steel with high welding speed. In Proceedings of the 5th International Symposium on Friction Stir Welding, Metz, France, 14–16 September 2004.
29. Tanaka, T.; Morishige, T.; Hirata, T. Comprehensive analysis of joint strength for dissimilar friction stir welds of mild steel to aluminum alloys. *Scr. Mater.* **2009**, *61*, 756–759. [CrossRef]
30. Takeoka, N.; Fujii, H.; Morisada, Y.; Sun, Y.F. Clarification of formation mechanism of stri zone using adjustable tool. In Proceedings of the 11th International Symposium on Friction Stir Welding, Cambridge, UK, 17–19 May 2016.
31. Murr, L.E. Intercalation vortices and related microstructural features in the friction stir welding of dissimilar metals. *Mater. Res. Innov.* **1998**, *2*, 150–153. [CrossRef]
32. Murr, L.E. A comparative study of friction stir welding of aluminum alloys. *Alum. Trans.* **1999**, *1*, 141–154.
33. Liu, F.C.; Ma, Z.Y. Influence of tool dimension and welding parameters on microstructure and mechanical properties of friction stir welded 6061-T651 aluminum alloy. *Metall. Mater. Trans. A* **2008**, *39*, 2378–2388. [CrossRef]
34. Sato, Y.S.; Kurihara, Y.; Pack, S.H.C.; Kokawa, H.; Tsuji, N. Friction stir welding of ultrafine grained Al alloy 1100 produced by accumulative roll-bonding. *Scr. Mater.* **2004**, *50*, 57–60. [CrossRef]
35. McQueen, H.J.; Knustad, O.; Ryum, N.; Solberg, J.K. Microstructural evolution in Al deformed to strains of 60 at 400 °C. *Scr. Metall.* **1985**, *19*, 73–78. [CrossRef]
36. Humphreys, F.J.; Hatherly, M. *Recrystallization and Related Annealing Phenomenon*; Pergamon Press: Oxford, UK, 2004.
37. McQueen, H.J.; Solberg, J.K.; Ryum, N.; Ness, E. Evolution of flow stress in Al during ultra-high straining at elevated temperature. *Philos. Mag. A* **1989**, *60*, 473–485. [CrossRef]